A Dynamic HRA Framework for Persistently Responding to Environmental Changes: A Preliminary Test of Competing Outcomes Sampling Using the Proposed Concurrent Continuous Markov Chain Monte Carlo (Co-CMMC) Method

Chun-Yen Li [a], and Yukihiro Kirimoto [a]
[a] Central Research Institute of Electric Power Industry, Kanagawa, Japan,
li40806@criepi.denken.or.jp

Abstract: Human Reliability Analysis (HRA) is a pivotal element in Probabilistic Risk Assessment (PRA) as it estimates human error probability (HEP) in human–machine activities such as repair. Conventional HRA methods link performance shaping factors (PSFs) to static, pre-defined scenarios, making it difficult to directly represent work contexts that evolve continuously. In contrast, the field of dynamic PRA provides a means to capture dynamic characteristics by stochastically generating event sequences that track time-varying machine behavior. Within this field, the Continuous Markov chain Monte Carlo (CMMC) method recalibrates state-transition probabilities at each time step using environment-responsive failure rates and advances the machine state through Monte Carlo sampling, yielding time-ordered machine state histories under persistent environmental variability. To account for maintenance, earlier CMMC extensions introduced repair activities by assuming a pairwise exchange between machine states and repair-task states (e.g., a failed state mapped to repair in progress, and an operating state mapped to repair completed), allowing repair histories to be inferred while simulating only the machine process. From an HRA viewpoint, however, repair termination is a competing-outcome process (success versus failure). This exchange assumption therefore obscures outcome-specific human performance and limits HEP estimation in dynamic environments. Afterwards, a Concurrent CMMC (Co-CMMC) method is proposed to realize a Dynamic HRA (DHRA) framework. In the Co-CMMC method, a joint Markov state that combines the machine state and repair-task states is defined, allowing both processes to evolve concurrently and stochastically without requiring pairwise exchanges. Consequently, by applying the Co-CMMC method, not only can the advantages of the original CMMC method be retained, but the competing outcomes of a dynamic repair task can also be sampled under the influence of dynamic human–machine–environment interactions. This capability highlights its potential for DHRA-oriented HEP estimation. This study aims to introduce the Co-CMMC-based DHRA framework and further demonstrate its practical application to a specific scenario through an assumed test case.

1. INTRODUCTION

Probabilistic Risk Assessment (PRA) is a fundamental methodology for evaluating complex safety and reliability issues in Nuclear Power Plants (NPPs). Within PRA, Human Reliability Analysis (HRA) plays an essential role in identifying potential human errors and quantifying their likelihood, commonly represented as Human Error Probability (HEP), during safety evaluations. However, conventional HRA methods are generally developed based on predefined and static scenarios. As a result, they have limited capability to capture the effects of transient environmental changes on operator performance. This limitation leads to persistent uncertainties when assessing human actions under dynamic accident conditions. To overcome the limitations of static accident representations, dynamic PRA (DPRA) approaches have been developed to explicitly model the temporal evolution and sequencing of events. These approaches enable a more comprehensive identification of possible failure pathways across different accident progressions. Such developments further emphasize the need for dynamic HRA methodologies that can account for time-dependent environmental influences on human performance while being consistently integrated into DPRA frameworks. Among DPRA methods, the CMMC method updates transition probabilities at each timestep using environment-dependent failure rates and advances system evolution through Monte Carlo sampling. In this way, it generates time-ordered histories of machine states under dynamically changing environmental conditions [1]. Previous studies have demonstrated the capability of CMMC to capture interactions between the environment and machine behavior. Moreover, its stepwise sampling mechanism provides high temporal resolution, making it particularly suitable for analyzing complex dynamic interactions, including not only machine–environment relationships but also human–machine–environment interactions.

Previous extensions of the CMMC method have introduced repair task modeling through a one-to-one correspondence between machine states and task states [1]. Under this representation, a machine failure state corresponds to a repair-in-progress state, whereas machine operation corresponds to repair completion. This formulation allows repair histories to be inferred directly from machine state trajectories. However, repair completion is inherently associated with competing outcomes, namely success and failure. Therefore, a simple one-to-one correspondence is insufficient for accurately representing outcome-dependent human performance. To address this limitation and support Dynamic HRA (DHRA), the authors' previous work proposed a Concurrent CMMC (Co-CMMC) method, in which the Markov state space is extended to a joint machine–repair task representation [2]. This formulation enables machine dynamics and repair task processes to evolve concurrently in a stochastic manner. Based on this method, a computational framework for DHRA was also developed to extract dynamic repair task histories under coupled human–machine–environment interactions. Building on this previous work, the present study introduces the Co-CMMC-based DHRA framework and demonstrates its practical application to a specific scenario through an assumed test case.

2. OVERVIEW OF CO-CMMC BASED DHRA FRAMEWORK

This section presents the proposed DHRA framework, which incorporates the Petri-net model and Co-CMMC method, for tracking repair tasks. The framework is designed to extract the dynamic history of repair activities under human–machine–environment interactions at a timestep-wise resolution.

The proposed DHRA framework consists of four modules. The conceptual execution sequence of these modules along the timeline is illustrated in Fig. 1. The four modules are defined as follows:

(1) Module 1: **Environmental Influence Interpretation Module**
(2) Module 2: **Stochastic Event-Transition Analysis Module**
(3) Module 3: **State Interpretation Module**
(4) Module 4: **Deterministic Environment-Transition Analysis Module**

As shown in Fig. 1, at each timestep, Module 1 first evaluates the influence of environmental conditions on component failure, as well as on the completion and success or failure of repair tasks. The processed results are then passed to Module 2, where stochastic event sampling is performed. Based on this process, for each component, the joint Markov state at the next timestep is determined by combining the state of executed repair task by the operator and the intrinsic state of the component. The Co-CMMC method is primarily applied in this stage. After all components have been processed in Module 2, Module 3 performs a decomposition of the joint Markov states. The component states are then introduced into the PN model to determine the corresponding system state among the multi-state space at the next timestep. Finally, Module 4 updates the environmental states deterministically, based on the current states of all components and systems, as well as the execution status of the associated repair tasks. This process is repeated iteratively until the predefined end time is reached. Although there is space limitations, further details of the Co-CMMC based DHRA framework can be found in [2].

Figure 1: Flowchart of Co-CMMC Based DHRA Framework

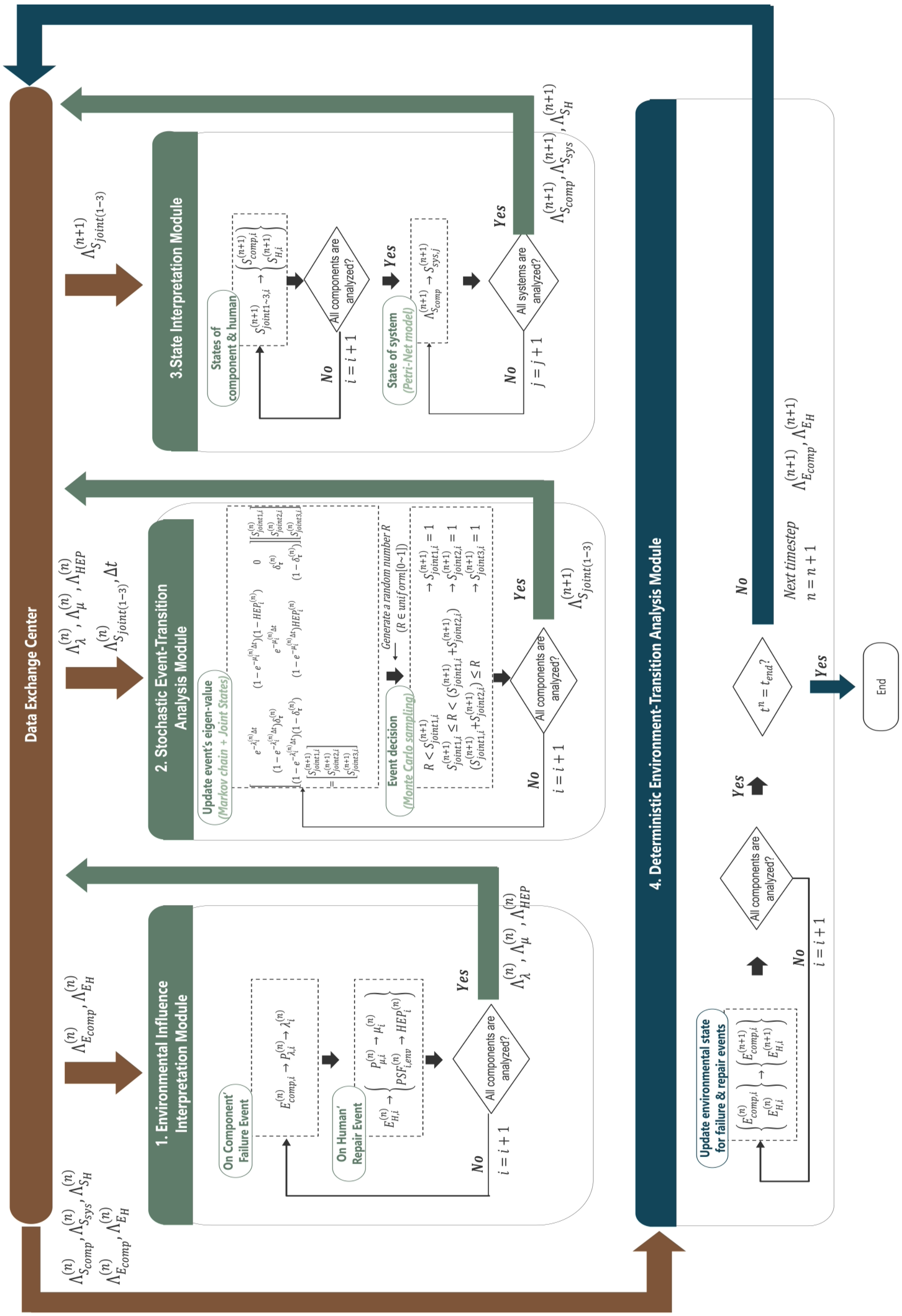

3. TEST SCENARIO DISCUSSION

3.1. Scenario Background

To examine the Co-CMMC based DHRA framework, this study employs a hypothetical scenario involving volcanic ashfall hazards affecting a typical sodium-cooled fast reactor (SFR), as illustrated in Fig. 2.

In the SFR, decay heat removal relies on the Auxiliary Cooling System (ACS), which operates through air cooling. The ACS can function in either Forced Circulation (FC) or Natural Circulation (NC) mode, where the FC mode requires electrical power supplied by the Electricity Distribution System (EDS). However, volcanic ash deposition may clog the ACS filters, potentially leading to system failure. In addition, ash accumulation can also impair the filters of the Emergency Diesel Generators (EDGs) and the Heating, Ventilation, and Air Conditioning (HVAC) system. The degradation of the EDGs and HVAC further influences the ability of the EDS to provide power to the ACS for FC mode operation.

To restore the decay heat removal capability, repair tasks can be performed to replace the malfunctioning filters. However, during the replacement process, the accumulated ash on the filters may be disturbed, dislodged, and subsequently dispersed into the surrounding work environment. The resulting increase of the ash concentration in the working environment reduces personnel visibility and may adversely affect human performance during the repair tasks.

The filter failure analysis is conducted in previous work [1]. Therefore, the following section primarily focuses on explaining the repair task (filter replacement) and how the repair task is applied to Co-CMMC based DHRA framework in this study.

Figure 2: Scheme of Volcanic Ashfall on SFR

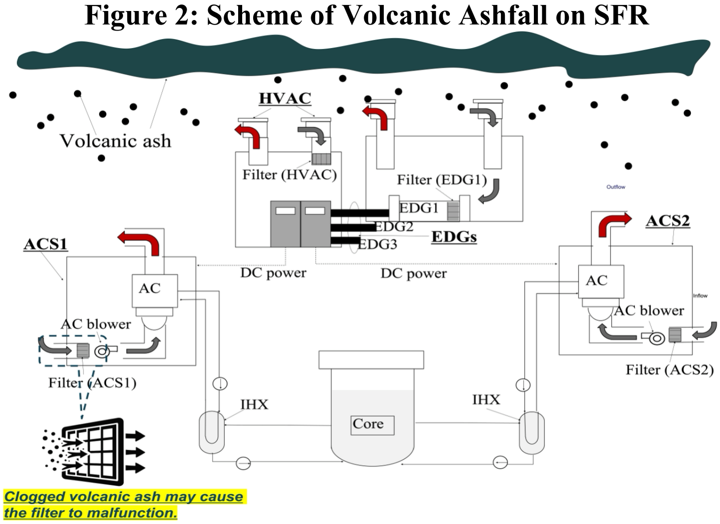

3.2. Application to Co-CMMC Based DHRA Framework

To apply the Co-CMMC-based DHRA framework to a specific scenario, it is necessary to construct the corresponding Markov chain structure and establish the relationships between the working environment, the HEP, and the associated $\mu_i^{(n)}$ parameters. Furthermore, a suitable approach for modeling the dynamics of the working environment is required. The implementation of these elements for the test scenario considered in this study is described in the following sections.

3.2.1 Relation between Repair Task and Markov Matrix Structure

In Module 2 of the Co-CMMC-based DHRA framework, the state updating of the joint Markov states, which represent the composite state of the component and its corresponding repair status, must rely on the structure of the Markov chain. Therefore, this section further discusses the repair task considered in the target scenario and demonstrates an example of the corresponding Markov chain structure.

First, the repair task considered in this study mainly consists of the following steps: opening the inspection hatch, inserting the isolation plate to prevent volcanic ash from entering during filter replacement, releasing the filter fasteners, removing the old filter, installing the new filter, re-securing the filter fasteners, removing the isolation plate, and closing the inspection hatch. During the installation of the new filter, attention must be paid to the airflow direction mark. It is also necessary to ensure that the filter is properly positioned so that the gasket is uniformly compressed, that the filter is pushed to the positioning stop, and that the surrounding gasket is not folded outward, curled, or showing any visible gaps.

In this scenario, the inspection hatch of the filter is assumed to be located in an indoor environment within the plant. Therefore, the filter repair task is assumed to be performed indoors. In addition, when the old filter is removed, volcanic ash deposited on the filter may fall into the working environment and disperse. The dispersed volcanic ash may reduce visibility, or the visible distance, and consequently affect the execution of the repair task. Furthermore, because the volcanic ashfall scenario is assumed to continue for 24 hours, even after the repair is completed, the repair task must be performed again if the filter loses its function once more. Regarding the influence of visibility on the repair task, volcanic ash suspended in the working environment may degrade visibility, making the steps that originally rely on visual judgment more prone to misjudgment or requiring the use of tactile cues as supplementary information. In this study, the removal of the old filter is regarded as the source that increases the volcanic ash concentration in the working environment. This causes a difference in the visibility-related PIF before and after the “removal of the old filter” step within the same repair task. Therefore, for the purpose of IDHEAS-ECA assessment, the repair task is divided into two sub-tasks. The steps from opening the inspection hatch to releasing the filter fasteners are defined as the “Pre-replacement Access and Isolation Task”, whereas the steps from removing the old filter to closing the inspection hatch are defined as the “Filter Removal, Installation, and Restoration Task.”

For the Pre-replacement Access and Isolation Task, except for the step of inserting the isolation plate, the other steps can still be completed with the aid of tactile cues even if visibility deteriorates. For example, even under poor visibility, the operator can still identify the positions of the inspection hatch or the fasteners by touch, or confirm whether the fasteners have been fully released. Therefore, the completion of these steps is relatively less problematic. However, for the step of inserting the isolation plate, visual judgment is required to determine whether the plate has been inserted into the correct position and to the proper depth. Although tactile cues may be used as supplementary information, the insertion position and depth do not provide sufficiently clear criteria for judgment. If the operator relies only on the perceived insertion resistance, misjudgment may occur. Therefore, visual confirmation is still necessary. Moreover, if the isolation plate is not fully inserted into the correct position, ash-laden air may enter the interior of the filter system during the subsequent filter replacement process. This may damage the fan of the air cooler or the generator located downstream of the filter, resulting in failure of the entire repair task.

For the Filter Removal, Installation, and Restoration Task, except for the step of installing the new filter, the other steps can still be completed with the aid of tactile cues even if visibility deteriorates. For example, under poor visibility, the operator can still locate the fasteners, re-secure the fasteners, or remove the isolation plate by touch. These steps are therefore considered relatively less problematic. However, for the step of installing the new filter, visual judgment is required to verify the airflow direction mark, to confirm whether the filter is correctly positioned so that the gasket is uniformly compressed, to ensure that the filter is pushed to the positioning stop, and to check that the surrounding gasket is not folded outward, curled, or showing visible gaps. These visual judgment requirements are prone to error under degraded visibility, and tactile cues may not provide significant assistance. As a result, when the isolation plate is removed and the new filter resumes operation, bypass flow or leakage may allow ash-laden air to enter the interior of the filter system. This may damage the fan of the air cooler or the generator located downstream of the filter, resulting in failure of the entire repair task.

In summary, the entire repair task is divided into two sub-tasks in this study: Task 1, the Pre-replacement Access and Isolation Task, and Task 2, the Filter Removal, Installation, and Restoration Task. The overall HFE is defined as follows: after the existing filter is known to have failed and the maintenance personnel have initiated the replacement task according to the established procedure, the repair task fails to successfully restore and maintain the filtration function required for the air-cooling system. The Markov chain structure corresponding to this setting is demonstrated in Fig. 3 and Table 1.

Figure 3: Markov Chain Structure for Describing Repair Task

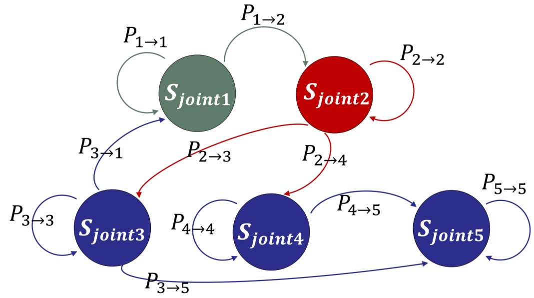

Table 1: Transition Probabilities Corresponding to Figure 3

	$P_{1\to}$	$P_{2\to}$	$P_{3\to}$	$P_{4\to}$	$P_{5\to}$
$P_{\to1}$	$e^{-\lambda_i^{(n)}\Delta t}$	0	$(1 - e^{-\mu_{i,task2}^{(n)}\Delta t})(1 - HEP_{i,task2}^{(n)})$	0	0
$P_{\to2}$	$1 - e^{-\lambda_i^{(n)}\Delta t}$	$e^{-\mu_{i,task1}^{(n)}\Delta t}$	0	0	0
$P_{\to3}$	0	$(1 - e^{-\mu_{i,task1}^{(n)}\Delta t})(1 - HEP_{i,task1}^{(n)})$	$e^{-\mu_{i,task2}^{(n)}\Delta t}$	0	0
$P_{\to4}$	0	$(1 - e^{-\mu_{i,task1}^{(n)}\Delta t})HEP_{i,task1}^{(n)}$	0	$e^{-\mu_{i,task2}^{(n)}\Delta t}$	0
$P_{\to5}$	0	0	$(1 - e^{-\mu_{i,task2}^{(n)}\Delta t})HEP_{i,task2}^{(n)}$	$1 - e^{-\mu_{i,task2}^{(n)}\Delta t}$	1

The corresponding joint Markov states are described as follows.

(1) $S_{joint1,i}^{(n)}$: the i_{th} component is working, and the repair task1&2 for the i_{th} component are stopped.
(2) $S_{joint2,i}^{(n)}$: the i_{th} component is stopped, and the repair task1 (Pre-replacement Access and Isolation Task) for the i_{th} component is undergoing.
(3) $S_{joint3,i}^{(n)}$: the i_{th} component is stopped, and the repair task1 for the i_{th} component is stopped with success, and the repair task2 (Filter Removal, Installation, and Restoration Task) is undergoing.
(4) $S_{joint4,i}^{(n)}$: the i_{th} component is stopped, and the repair task1 for the i_{th} component is stopped without success, and the repair task2 is undergoing.
(5) $S_{joint5,i}^{(n)}$: the i_{th} component is stopped, and the repair task1&2 for the i_{th} component are stopped. Either task1 or task2 is without success.

As illustrated in Fig. 3, whether the failure occurs in Task 1 $\left(S_{joint2,l}^{(n)} \rightarrow S_{joint4,l}^{(n+1)}\right)$or in Task 2 $\left(S_{joint3,l}^{(n)} \rightarrow S_{joint5,l}^{(n+1)}\ or\ S_{joint4,l}^{(n)} \rightarrow S_{joint5,l}^{(n+1)}\right)$, the system eventually transitions to $S_{joint5,l}^{(n+1)}$ after the execution of the two tasks. Once this state is reached, the machine remains stopped and is no longer subject to further repair.

3.2.2 Relation between Working Environment and HEP

In Module 1, because the HEP must be updated at each timestep based on the current working environment, this section first derives the HEP calculation formulas for Task 1 and Task 2 according to the test scenario considered here, and then links the HEP with the working-environment parameters. In addition, because the HEP used in this framework conceptually separates failure-contributing factors related to task duration from other factors, IDHEAS-ECA [3] is used for the analysis, and its P_c is adopted as the HEP to be incorporated into this study's DHRA framework.

First, the considerations for selecting the Cognitive Failure Modes (CFMs) for Task 1 and Task 2 are summarized in Table 2. This study does not include the detection of filter failure, the understanding of alarms, or the selection of repair strategies within the HFE boundary. Instead, the HFE is limited to the "failure to execute a predefined repair task." In other words, the starting point of the HFE is not "the abnormal condition is detected" or "the situation is diagnosed," but rather "the maintenance worker has already obtained the predefined repair plan and has begun execution." Therefore, among the five CFMs, only CFM4, failure of action execution, is selected as the target for quantification, while detection, understanding, decision-making, and inter-team coordination are not selected.

The PIF values selected for the two tasks and the corresponding considerations are also summarized in Table 3. The base PIFs for the two critical tasks are first evaluated based on Scenario Familiarity and Task Complexity. Since the maintenance worker is assumed to be professionally trained, and the HFE boundary has been narrowed to the execution of predefined maintenance procedures, both critical tasks are assigned SF0 for scenario familiarity. For Task Complexity, the Pre-replacement Access and Isolation Task, Task 1, is assigned C30 because its execution path is short, linear, and involves only a few steps; the main source of risk does not lie in the complexity of the step sequence itself. The Filter Removal, Installation, and Restoration Task, Task 2, is assigned C31 because it is still a straightforward procedure-execution task, but it involves a noticeably larger number of sequential steps, and after the new filter is inserted, a set of installation acceptance criteria must also be confirmed.

Among the modification PIFs, visibility is represented by the Environmental PIF. When the visible distance is low enough that key visual confirmations cannot be performed reliably, ENV6 is assigned; otherwise, ENV0 is assigned. For Physical Demands, Task 1 is assigned PD0, whereas Task 2 is assigned PD2, because inserting the new filter and confirming the sealing condition require higher spatial precision. Under the baseline boundary conditions of this study, all other modification PIFs are assigned no-impact attributes.

Table 2: Typeset of Papers

CFM	Task1	Basis for Judgment	Task2	Basis for Judgment
Detection (D)	Not required	The initiation condition for the repair task is determined by an external model and maintenance management. Local visual confirmation is treated as verification of execution outcomes and is not modeled separately as cue detection.	Not required	Same as the Pre-replacement task; visual confirmation during new filter insertion is treated as verification of execution outcomes.
Understanding (U)	Not required	The task does not require integrating multiple pieces of system information to form situational understanding. It only requires confirming whether the closure plate has reached the correct position under a predefined procedure.	Not required	The task does not require diagnosing the equipment status. It only requires confirming the seating and sealing condition of the new filter according to predefined criteria.
Decision making (DM)	Not required	The task does not involve deciding whether to perform the repair or whether to select an alternative strategy. The repair method is predefined.	Not required	The task does not involve strategy selection. It only requires correct execution according to the predefined procedure.
Action Execution (E)	Required	The task includes procedural execution and outcome verification, such as inserting the closure plate, confirming its position and insertion depth, and releasing the filter fasteners.	Required	The task includes procedural execution and outcome verification, such as removing the old filter, inserting the new filter, confirming the airflow direction, stop position, gasket condition, and absence of visible gaps, and restoring the system configuration.
Interteam Coordination (T)	Not required	The problem setting does not specify cross-team	Not required	Same as the Pre-replacement task.

	command, authorization, or resource coordination.	

Table 3: Typeset of Papers

PIF	Task1	Selection Rationale	Task2	Selection Rationale
Scenario Familiarity	SF0, base HEP = 0	The HFE boundary is restricted to the direct execution of a predefined maintenance procedure. For trained maintenance personnel, this is a familiar procedural execution task rather than an unfamiliar diagnostic situation.	SF0, base HEP = 0	Same as the Pre-replacement task. Although volcanic ash is an external scenario condition, this sub-task itself remains the execution of a predefined filter replacement procedure.
Information Availability and Reliability	N/A for CFM (E)	The CFM (E) worksheet in [3] explicitly indicates that this base PIF is not used for action execution.	N/A for CFM (E)	Same as the Pre-replacement task.
Task Complexity	C30, base HEP = 0	The task is linear, has only a few steps, follows a single execution path, and does not involve multiple interleaved procedures. The dominant contributor to risk is not procedural complexity.	C31, base HEP = 1.00E-03	The task is still a straightforward procedure, but it involves more steps and includes multiple post-installation confirmation items.
Environmental PIFs	ENV0 to ENV6 (w =1~ 5)	In the indoor work area, the dominant environmental challenge is reduced visibility caused by volcanic ash. If visibility becomes too low to reliably judge the closure plate position or insertion depth, ENV6 is selected.	ENV0 to ENV6 (w =1~ 5)	After the old filter is removed, volcanic ash may disperse further into the work area. If visibility becomes too low to reliably identify the airflow marking, gasket condition, stop position, or visible gaps, ENV6 is selected.
System and I&C Transparency	SIC0 (w = 1)	This is a local mechanical replacement task and does not involve opaque system logic or reset behavior.	SIC0 (w = 1)	Same as the Pre-replacement task.
Human-System Interface	HSI0 (w = 1)	The baseline assumption is that the inspection opening, closure plate, fasteners, markings, and positioning interface are normally designed. The visibility issue is already represented by the Environmental PIF and is not double counted here.	HSI0 (w = 1)	The baseline assumption is that the airflow arrow, positioning stop, and visual inspection interface can be normally identified. Additional weighting is not applied again for visibility under HSI.
Equipment and Tools	TP0 (w = 1)	The closure plate, fasteners, and necessary tools or spare parts are available under normal administrative control.	TP0 (w = 1)	The new filter, fasteners, and tools are available under normal administrative control.
Staffing	STA0 (w = 1)	The problem setting does not include additional assumptions such as staffing shortage, unclear roles, or lack of peer checking.	STA0 (w = 1)	Same as the Pre-replacement task.
Procedures, Guidance, and Instructions	PG0 (w = 1)	The baseline assumption is that a maintenance procedure exists and is sufficient to guide the task. PG2 or PG4 should be considered only if the actual procedure describes the closure plate positioning criteria ambiguously.	PG0 (w = 1)	The problem statement already provides explicit installation acceptance criteria. Therefore, no additional procedure-related penalty is applied in the baseline analysis.
Training	TE0 (w = 1)	The problem statement explicitly states that the maintenance personnel are professionally trained. Since there is no evidence of insufficient training frequency, TE1 is not selected.	TE0 (w = 1)	Same as the Pre-replacement task.
Teamwork and Organizational Factors	TF0 (w = 1)	The problem setting does not specify deficiencies in team composition, command structure, or cross-team information management.	TF0 (w = 1)	Same as the Pre-replacement task.
Work Processes	WP0 (w = 1)	No issues are assumed regarding self-checking, supervision, briefing, or other work process controls.	WP0 (w = 1)	Same as the Pre-replacement task.
Multitasking, Interruption, and Distraction	MT0 (w = 1)	The problem setting treats the repair task as a direct execution task and does not include concurrent scenario-management activities.	MT0 (w = 1)	Same as the Pre-replacement task.

Mental Fatigue and Time Pressure and Stress	MF0 (w = 1)	The problem statement does not provide information indicating a tight time window, prolonged high-cognitive workload, or emotional stress. Therefore, the baseline evaluation applies no additional weighting.	MF0 (w = 1)	Same as the Pre-replacement task.
Physical Demands	PD0 (w = 1)	The main challenge is visibility, not high-precision control or high-force physical work.	PD2 (w = 2)	Comparing with inserting temporary isolation plate, inserting and confirming the sealing condition of the new filter requires high spatial precision, which is consistent with PD2.
Recovery Factor	R = 1	The problem setting does not provide a clearly defined recovery mechanism that can reliably identify and correct an error after it occurs and before the HFE endpoint.	R = 1	Same as the Pre-replacement task.

Based on Tables 2 and Tables 3 above, $P_{i,\mathrm{CFMBASE},task1}$ and $P_{i,\mathrm{CFMBASE},task2}$ can be estimated separately in Table 4. Once $P_{i,\mathrm{CFMBASE},task1}$ and $P_{i,\mathrm{CFMBASE},task2}$ are obtained, the P_c values for the respective tasks can be determined according to the corresponding PIF settings. For $HEP_i^{(n)}$ used in the DHRA framework of this study, because the design concept is intended to isolate the contribution of P_t, the estimation of $HEP_{i,task1}^{(n)}$ and $HEP_{i,task2}^{(n)}$ only adopts the P_c component from IDHEAS-ECA, as shown in Eq. 1 and Eq. 2.

$$HEP_{i,task1}^{(n)} = P_{i,CFMBASE,task1}[PIF_{i,ENV}^{(n)}] \tag{1}$$

$$HEP_{i,task2}^{(n)} = P_{i,CFMBASE,task2}[1 + PIF_{i,ENV}^{(n)}] \tag{2}$$

Table 4: P_{CFMBASE} Estimation for Task1 and Task2

Item	Task1	Task2
Scenario Familiarity	SF0 = 0	SF0 = 0
Information Availability and Reliability	N/A	N/A
Task Complexity	C30 = 0	C31 = 1.00E-03
Base HEP lower bound for CFM4	1.00E-04	1.00E-04
P_{CFMBASE}	1.00E-04	1.00E-03

In Eq. 1 and Eq. 2, $PIF_{i,\mathrm{ENV}}^{(n)}$ is used here as an interface for dynamically establishing the relationship with the working environment, and is linked to visibility. Although no experimental data are currently available, this study assumes that when visibility is less than or equal to the arm length required for manual work, set here as 1 m, the maximum penalty of $PIF_{i,\mathrm{ENV}}^{(n)} = 5$ is assigned. As visibility increases, $PIF_{i,\mathrm{ENV}}^{(n)}$ gradually decreases, until the visibility range exceeds the distance at which the surrounding contours can be clearly perceived, set here as 6 m. Beyond this range, $PIF_{i,\mathrm{ENV}}^{(n)}$ is set to 1, as expressed in the following equations.

$$PIF_{i,ENV}^{(n)} = 5\ [if\ VIS_i^{(n)} < 1m] \tag{3}$$

$$PIF_{i,ENV}^{(n)} = 1\ [if\ VIS_i^{(n)} > 6m] \tag{4}$$

$$PIF_{i,ENV}^{(n)} = 5e^{-\frac{\ln 5}{5}(VIS_i^n - 1)}\ [if\ 1\mathrm{m} \le VIS_i^{(n)} \le 6m] \tag{5}$$

The relationships between $VIS_i^{(n)}$ and $PIF_{i,\mathrm{ENV}}^{(n)}$, $HEP_{i,\mathrm{task1}}^{(n)}$, and $HEP_{i,\mathrm{task2}}^{(n)}$, respectively, are also summarized in Fig. 4.

Finally, $VIS_i^{(n)}$ can be estimated using the ash mass concentration at the current location of the repair worker. Visibility is typically expressed as follows:

$$\mathrm{VIS}_i^{(n)} = 3.912/\beta_{ext,i}^{(n)} \tag{6}$$

where $\beta_{ext,i}^{(n)}$ [1/m] represents the extinction coefficient corresponding to ash mass concentration where the repair man is. When the diameter of the volcanic ash particles is significantly larger than the wavelength of visible light, the geometric scattering approximation can be applied, allowing $\beta_{ext,i}^{(n)}$ to be expressed as follows:

$$\beta_{ext,i}^{(n)} = 2\pi \sum_p r_p^2 n_{i,r_p}^{(n)} \tag{7}$$

where $n_{i,r_p}^{(n)}$ [1/m^3] denotes the number density of ash particles with radius r_p during the repair of the i_{th} SSC at the n_{th} timestep. Accordingly, the impact of ash mass concentration on $VIS_i^{(n)}$ can be estimated by applying the information of ash mass concentration from Module 4 to $\sum_p r_p^2 n_{i,r_p}^{(n)}$ in Eq. 7. From the above, it can be seen that the relationship between changes in the dynamic working environment, represented by ash mass concentration, and HEP is established through $VIS_i^{(n)}$.

Figure 4: Relation between $VIS_i^{(n)}$ and $PIF_{i,ENV}^{(n)}$ and $HEP_{i,}^{(n)}$ for Task1 and Task2

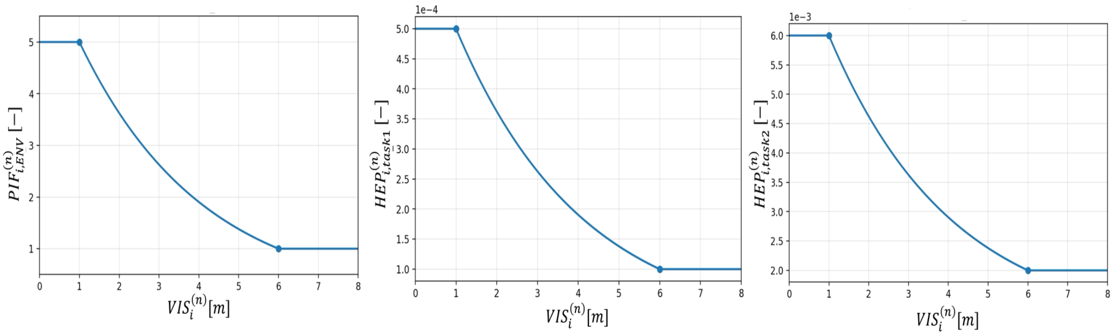

3.2.3 Relation between Working Environment and $\mu_i^{(n)}$

In Module 1, since $\mu_i^{(n)}$ must be updated at each timestep based on the current working environment, this section first derives the relationship between $\mu_i^{(n)}$ and the working-environment parameters based on the test scenario considered here.

First, when deriving $\mu_i^{(n)}$ corresponding to the working environment for Task 1 and Task 2, in this study's DHRA framework, it designed to referring Eq. 8 [2], which is based on the Erlang distribution. In addition to inputting the current time $t^{(n)}$ and the k value corresponding to each task, the timestep-dependent $\beta_i^{(n)}$ is also required. Here, $\beta_i^{(n)}$ can be calculated through Eq. 9 [2] using the corresponding $P_{\mu,i}^{(n)}$ and $T_{g,i}$ at that timestep.

$$\mu_i^{(n)} = \frac{PDF_{Erlang\ distribution}}{1-CDF_{Erlang\ distribution}} = \frac{(\beta_i^{(n)})^k (t^{(n)})^{k-1}/(k-1)!}{\sum_{l=0}^{k-1} \frac{(\beta_i^{(n)} \times t^{(n)})^l}{l!}} \tag{8}$$

$$P_{\mu,i}^{(n)} = 1 - e^{-\beta_i^{(n)} \times (T_{g,i})} \sum_{l=0}^{k-1} \frac{(\beta_i^{(n)} \times T_{g,i})^l}{l!} \tag{9}$$

For $T_{g,i}$, historical data or CFD analysis would generally be required for evaluation. However, because complete corresponding data are not currently available, an estimation approach is adopted here to derive the values of $T_{g,i}$ for application. Referring to the reference data on the time required for filter replacement work, this study assumes a path in which the entire repair task requires an average of 60 minutes, and this duration is evenly distributed among the individual steps: Task 1 consists of 3 steps, while Task 2 consists of 5 steps, as described in section 3.2.1. It is further assumed that there is a 0.95 probability that the repair work for each task can be completed within its respective $T_{g,i}$. Based on this assumption, Eq. 9 is used to estimate each $T_{g,i}$, and the results are shown in the following table.

Table 5: $T_{g,i}$ Estimation for Task1 and Task2

Task	Conditions	Equation and solution for $x = \beta_i\ T_{g,i}$	Calculation of $T_{g,i}$
Task1	• $P_{\mu,i} = 0.95$ • $\beta_i = \frac{1}{60/8} = \frac{1}{7.5} = 0.1333$ • $k = 3$	Let $x = \beta_i\ T_{g,i}$, then $1 - e^{-x}(1 + x + \frac{x^2}{2}) = 0.95$. Solving gives $x \approx 6.2958$	$T_{g,i,task1} = \frac{x}{\beta_i} \approx 47.2197\ [min]$
Task2	• $P_{\mu,i} = 0.95$ • $\beta_i = \frac{1}{60/8} = \frac{1}{7.5} = 0.1333$ • $k = 5$	Let $x = \beta_i\ T_{g,i}$, then $1 - e^{-x}\sum_{l=0}^{4}\frac{x^l}{l!} = 0.95$. Solving gives $x \approx 9.1535$	$T_{g,i,task2} = \frac{x}{\beta_i} \approx 68.6684\ [min]$

Next, $P_{\mu,i}^{(n)}$ serves as the interface for establishing the linkage with the working environment. Therefore, in this scenario, the variation in $VIS_i^{(n)}$, which is the primary environmental factor considered, is adopted as the variable for constructing the assumed relationship.

$$P_{\mu,i}^{(n)} = 1 - e^{-\mathrm{VIS}_i^{(n)} C_{VIS}} \tag{10}$$

In this study, C_{VIS} is set to 2.9957, under the assumption that $P_{\mu,i}^{(n)} = 0.95$ when $\mathrm{VIS}_i^{(n)} = 1$. The relationship between $P_{\mu,i}^{(n)}$ and $\mathrm{VIS}_i^{(n)}$ can be expressed as shown in the following figure.

Figure 5: The Relation between $\mathrm{VIS}_i^{(n)}$ and $P_{\mu,i}^{(n)}$

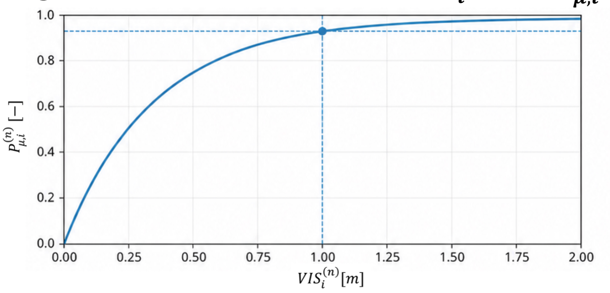

Based on the estimated values of $T_{g,i,\mathrm{task1}}$ and $T_{g,i,\mathrm{task2}}$, the relationship between $P_{\mu,i}^{(n)}$ and $\mathrm{VIS}_i^{(n)}$, and the k values assigned to Task 1 and Task 2, respectively, these parameters can then be substituted into Eq. 8 and Eq. 9. Accordingly, the relationships of $t^{(n)}$ and $\mathrm{VIS}_i^{(n)}$ with $\mu_{i,\mathrm{task1}}^{(n)}$ and $\mu_{i,\mathrm{task2}}^{(n)}$ can be obtained, as shown in the following figure.

Figure 6: The Relation between $\mathrm{VIS}_i^{(n)}$, $t^{(n)}$, and $\mu_i^{(n)}$ for Task1 and Task2.

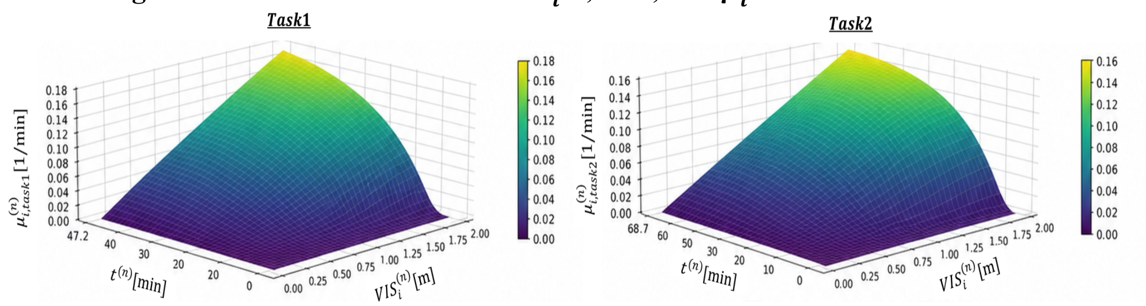

Since $\mathrm{VIS}_i^{(n)}$ can be inferred from the ash mass concentration information described in Section 3.2.2, the relationship between the dynamic variation of the working environment and $\mu_i^{(n)}$ is thus established.

3.2.4 Simulation of Working Environment

Since the analyses in Sections 3.2.2 and 3.2.3 both require information on ash mass concentration to estimate visibility, $VIS_i^{(n)}$, this section mainly describes the procedure used in Module 4 to dynamically estimate ash mass concentration in the working environment. Specifically, it considers the diffusion of volcanic ash dislodged from the filter during Task 2 throughout the working-environment space.

In this study, Fick's first law is applied to the continuity equation to model the diffusion process of the dislodged ash. Consequently, the spatiotemporal-dependent ash mass concentration, $c(r,t)$ [kg/m^3] is governed by the following equation:

$$\frac{\partial c(r,t)}{\partial t} = D\nabla^2 c(r,t) + S(r,t) \quad [r \in \mathbb{R}^3, t > 0] \tag{11}$$

where D [m^2/s] is diffusivity constant, and $S(r,t)$ represents the source term for volcanic ash generation or absorption. Since the dislodged ash from the malfunctioning filter should be considered as $S(r,t)$, a simplification is made by assuming that the dislodged ash is released instantaneously at the beginning of the task rather than continuously over time. Under this assumption, $S(r,t)$ is set to zero, and the initial released ash mass concentration M_0 [kg/m^2] around the released location r_0 is defined as the initial condition. Meanwhile, at an infinite distance from the point of ash release, the ash concentration is assumed to be zero as the boundary condition. For a three-dimensional infinite domain, the classical analytical solution for $c(r,t)$ under the given conditions is as below:

$$c(r,t) = \frac{M_0}{(4\pi Dt)^{1/2}} e^{\left(\frac{-\|r-r_0\|^2}{4Dt}\right)} \quad [t > 0] \tag{12}$$

In this study, r_0 is set as 0. Furthermore, considering the repetitive nature of the repair task, the contribution of all previously released ash masses can be treated as a linear superposition. Consequently, the expression for $c(r,t)$ is expanded to:

$$c_i^{(n)} = \sum_{M=1}^{m} H\left(t_i^n - t_{i,M(start)}\right) \times \frac{M_{i,M}}{\left[4\pi D\left(t_i^n - t_{i,M(start)}\right)\right]^{\frac{1}{2}}} \times e^{\left(\frac{-\|r_i^n\|^2}{4D\left(t_i^n - t_{i,M(start)}\right)}\right)} \tag{13}$$

where c_i^n [kg/m^3] means the ash mass concentration when repairing i_{th} component at n_{th} timestep, and $t_{i,M(start)}$ [s] means the starting time of the M_{th} repair task for i_{th} component, and m means the order of the current task when repairing i_{th} component at n_{th} timestep. $H(\cdot)$ is the Heaviside step function ensuring that contributions from previous repair tasks are only considered when $t_i^n > t_{i,M(start)}$. $M_{i,M}$ [kg/m^2] is the released ash mass concentration from the M_{th} repair task. By setting the radial distance between the dislodged ash and the staff position as r_i^n[m], c_i^n at each timestep can be determined by using Eq. 13 within Module 4.

4. CONCLUSION

To demonstrate the feasibility of the proposed Co-CMMC-based DHRA framework, which was developed in the authors' previous work to model stochastic human–machine–environment interactions, this study presents how to construct the corresponding Markov chain structure for a specific test case. It also establishes the relationships among the working environment, HEP, and the associated $\mu_i^{(n)}$parameters. These elements are required when applying the Co-CMMC-based DHRA framework and must be redesigned according to the target scenario. Future work will implement the settings provided in this study into computational code and conduct numerical analyses to further confirm the utility of the proposed framework.

References

[1] C. Y. Li, A. Watanabe, A. Uchibori and Y. Okano, "The Development of Petri Net-based Continuous Markov Chain Monte Carlo Methodology Applying to Dynamic Probability Risk Assessment for Multi-state Resilience Systems with Repairable Multi-component Interdependency under Longtermly Thereat," Journal of Nuclear Science and Technology, 61 (7), 935–957 (2024).

[2] C. Y. Li and Y. Kirimoto, "A Dynamic HRA Framework for Persistently Responding to Environmental Changes: Applying the Conceptual Proposal of the Concurrently Continuous Markov Chain Monte Carlo (Co-CMMC) Method for Sampling Competing Outcomes" NUTHOS-15 (2026).

[3] J. XING, Y. J. CHANG, J. D. SEGARRA. "Integrated human event analysis system for event and condition assessment (IDHEAS-ECA)," NUREG-2256[R]. US: Nuclear Regulatory Commission (2022).